Supplementary Information (SI) for Dalton Transactions.
This journal is © The Royal Society of Chemistry 2025

Supporting Information

Facile Synthesis of a Ru-based Polyoxometalate for Efficient Reduction of Nitrobenzene

Shihao Zhang, Yahao Sun, Wenjing Chen, Huafeng Li, Kunhong Li, Pengtao Ma, Jingping Wang*, Jingyang Niu*

Henan Key Laboratory of Polyoxometalate Chemistry, College of Chemistry and Molecular Sciences, Henan University, Kaifeng, 475004, Henan, P. R. China

Contents

Materials and Methods

All chemicals were obtained from commercial sources and used without further purification. Fourier transform infrared spectroscopy (FTIR) spectra were recorded on a Bruker VERTEX 70 using KBr tables in the range of 500–4000 cm^{-1}. The X–ray powder diffractometer (Bruker, D8 Advance) was used to record X–ray powder diffraction (PXRD) patterns in the 2θ angular range of 5−50° under Cu Kα radiation. The U–4100 spectrophotometer was used to measure UV/vis absorption spectra at room temperature. The amount of free water molecules was calculated by thermogravimetric analyses (TGA) on a Mettler–Toledo TGA/SDTA 851e instrument with a heating rate of 10 °C min^{-1} heated from 25 to 800 °C. On a Bruker 450–GC with a flame ionization detector and a 30 m column with nitrogen as the carrier gas, GC–MS (Agilent 7890B GC/5973B MS, SE–54 capillary column) and GC analyses were performed. The Bruker AVANCE NEO 500 MHz NMR spectrometer was used to record ^{1}H and ^{13}C NMR spectra.

X–ray crystallography

A single crystal of compound **1** was carefully selected under a microscope and the data collected on a Bruker D8 VENTURE PHOTON II CCD diffractometer with Mo Kα radiation source (the value of λ is 0.71073 Å). The SHELX structure program was used to determine the crystal structure, and refined by the full–matrix least–squares algorithm on F2 data using the ShelXL–2018/3 package within Olex2[1,2]. The C, N, O, P, Ru, W, Cl, and Na atoms were refined anisotropically in the final refinement cycle. And the amount of water molecules were calculated by TGA data. Crystallographic data and structural refinement parameters for compound **1** were listed in Table S1, with CCDC number: 2367306.

Table S1 Crystallographic data structure refinement for compound **1**

Compound	**1**
Empirical formula	$C_{20}H_{38}Cl_2N_4NaO_{50}PRu_2W_{11}$
Formula weight	3483.89
temperature (K)	150
Crystal system	triclinic
Space group	*p*-1
a/Å	13.7139(5)
b/Å	13.8151(5)
c/Å	23.4730(9)
α/°	89.7310(10)
β/°	76.2710(10)
γ/°	63.0070(10)
Volume/Å^3	3822.1(2)
Z	2
ρcalcg/cm^3	3.027
μ/mm^{-1}	17.044
F (000)	3096.0
Crystal size/mm^3	0.08 × 0.04 × 0.04
Radiation	Mo Kα (λ = 0.71073)
2θ range for data collection/°	4.604 to 50.194
Index ranges	-15 ≤ h ≤ 16, -16 ≤ k ≤ 16, -28 ≤ l ≤ 28
Reflections collected	47946
Independent reflections	13572 [R_{int} = 0.0717, Rsigma = 0.0722]
Data/restraints/parameters	13572/18/757
Goodness-of-fit on F^2	1.012
Final R indexes [I>=2σ (I)]	R_1 = 0.0436, wR_2 = 0.0830
Final R indexes [all data]	R_1 = 0.0747, wR_2 = 0.0947
Largest diff. peak/hole / e Å^{-3}	1.97/-2.27

[a] $R_1 = \sum||F_o| - |F_c||/\sum|F_o|$. [b] $wR_2 = [\sum w(F_o^2 - F_c^2)^2/\sum w(F_o^2)^2]^{1/2}$; $w = 1/[\sigma^2(F_o^2)+(xP)^2 + yP]$

Table S2 Selected bond distances (Å) for polyanion **1a**

Bond	Length (Å)	Bond	Length (Å)	Bond	Length (Å)
W1–O19	1.929(11)	W7–O26	1.921(13)	W5–O19	1.890(11)
W1–O17	1.888(11)	W7–O38	1.954(12)	W5–O20	1.683(11)
W1–O31	2.019(11)	W8–O23	1.955(12)	W6–O13	1.879(11)
W1–O9	1.714(12)	W8–O40	1.686(11)	W6–O15	1.858(13)
W1–O22	2.455(12)	W8–O24	2.472(12)	W6–O39	2.438(13)
W1–O5	1.785(11)	W8–O30	1.955(11)	W6–O26	1.878(13)
W2–O8	1.926(11)	W8–O18	1.828(11)	W6–O27	1.946(12)
W2–O6	1.703(10)	W8–O21	1.867(11)	W6–O16	1.704(12)
W2–O18	2.009(11)	W9–O34	1.714(11)	W7–O25	1.699(11)
W2–O10	1.969(12)	W9–O33	1.886(13)	W7–O12	1.810(11)
W2–O4	1.769(11)	W9–O32	1.892(11)	W7–O23	1.912(12)
W2–O11	2.372(10)	W9–O31	1.861(13)	P1–O24	1.556(12)
W3–O13	1.919(11)	W9–O36	1.900(13)	Ru1–N1	2.044(12)
W3–O12	2.033(11)	W10–O36	1.881(13)	Ru1–O5	2.001(11)
W3–O11	2.348(11)	W10–O29	1.858(13)	Ru2–O2	2.012(10)
W3–O8	1.915(10)	W10–O28	1.71(1)	Ru2–O1	1.807(10)
W3–O7	1.710(11)	W10–O37	1.904(12)	Ru2–Cl2	2.345(5)
W3–O2	1.784(10)	W10–O27	1.897(13)	Ru2–N4	2.031(13)
W4–O17	1.877(12)	W11–O37	1.911(12)	Ru2–O3	2.000(11)
W4–O14	1.697(12)	W11–O24	2.416(12)	Ru2–N3	2.058(13)
W4–O39	2.436(12)	W11–O30	1.886(12)	Ru1–Cl1	2.317(5)
W4–O3	1.804(11)	W11–O38	1.882(13)	P1–O39	1.495(11)
W4–O29	2.046(11)	W11–O35	1.685(13)	P1–O22	1.493(12)
W4–O15	1.983(12)	W11–O33	1.910(12)	P1–O11	1.547(11)
W5–O32	1.948(11)	Ru1–Cl1	2.317(5)	W5–O10	1.822(11)
W5–O22	2.456(11)	Ru1–N2	2.030(13)	Ru1–O4	2.008(11)
W5–O21	1.915(12)	Ru1–O1	1.806(10)		

Table S3 Selected bond angle (°) for polyanion **1a**.

Bond	Angle	Bond	Angle	Bond	Angle
N1–Ru1–Cl1	92.4(3)	N2–Ru1–Cl1	90.8(4)	N2–Ru1–N1	79.6(5)
O1–Ru1–Cl1	178.0(3)	O1–Ru1–N1	88.7(5)	O1–Ru1–N2	91.1(5)
O1–Ru1–O4	91.1(5)	O1–Ru1–O5	89.4(4)	O4–Ru1–Cl1	88.1(3)
O4–Ru1–N1	172.9(5)	O4–Ru1–N2	93.3(5)	O5–Ru1–Cl1	88.7(3)
N4–Ru2–Cl2	92.7(4)	N4–Ru2–N3	81.0(5)	O1–Ru2–Cl2	177.4(3)
O1–Ru2–N3	89.9(5)	O1–Ru2–N4	84.9(5)	O1–Ru2–O2	91.5(4)
O1–Ru2–O3	90.9(4)	O2–Ru2–Cl2	87.8(3)	O2–Ru2–N3	174.3(5)
O2–Ru2–N4	93.6(5)	O3–Ru2–Cl2	91.6(3)	O3–Ru2–N3	96.4(5)
O11–P1–O24	108.9(6)	O22–P1–O11	110.2(7)	O22–P1–O24	107.9(7)
O22–P1–O39	111.5(7)	O39–P1–O11	109.2(6)	O39–P1–O24	109.1(7)
O9–W1–O19	102.2(6)	O9–W1–O31	95.0(6)	O17–W1–O22	82.9(5)
O4–W2–O8	96.4(5)	O4–W2–O11	82.7(5)	O6–W2–O8	100.4(5)
O7–W3–O12	95.4(5)	O8–W3–O11	70.2(4)	O8–W3–O12	85.6(5)
O3–W4–O17	96.0(5)	O3–W4–O39	93.3(5)	O14–W4–O15	102.2(6)
O20–W5–O19	101.1(6)	O20–W5–O22	168.0(5)	O21–W5–O22	85.1(5)
O13–W6–O27	156.2(5)	O15–W6–O13	91.9(5)	O15–W6–O26	158.0(6)
O12–W7–O23	90.4(5)	O12–W7–O26	89.3(5)	O23–W7–O24	72.0(5)
O18–W8–O21	89.4(5)	O18–W8–O24	85.7(5)	O21–W8–O23	156.2(5)
O31–W9–O32	89.7(5)	O31–W9–O36	87.4(6)	O33–W9–O32	84.8(5)
O28–W10–O36	104.6(6)	O29–W10–O27	89.3(6)	O36–W10–O27	155.1(5)
O35–W11–O33	104.1(6)	O35–W11–O38	101.3(7)	O38–W11–O30	87.5(5)

Table S4 Bond valence sum (BVS) calculations of Ru, P, W and O atoms in **1a**.

Atom	BVS	Atom	BVS	Atom	BVS
W1	6.269	O7	1.769	O26	2.123
W2	6.259	O8	2.003	O27	2.002
W3	6.293	O9	1.750	O28	1.769
W4	6.138	O10	2.185	O29	1.899
W5	6.478	O11	1.777	O30	2.011
W6	6.409	O12	2.089	O31	1.943
W7	6.355	O13	2.126	O32	2.011
W8	6.380	O14	1.832	O33	2.129
W9	6.165	O15	2.031	O34	1.750
W10	6.183	O16	1.798	O35	1.892
W11	6.423	O17	2.220	O36	2.173
Ru1	4.398	O18	2.074	O37	2.074
Ru2	4.310	O19	2.066	O38	2.026
O1	2.154	O20	1.903	O39	1.838
O2	2.066	O21	2.173	O40	1.887
O2	3.628	O22	1.822	P1	4.998
O4	2.133	O23	1.937	O6	1.803
O5	2.081	O24	1.870	O25	1.822

Table S5 Optimization of **1** for reduction of nitrobenzene to aniline

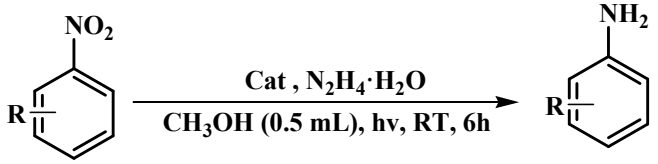

Entry	Catalyst (mg)	Solvent	Yield (%)
1	5	methanol	99.8
2	5	acetonitrile	55.8
3	5	chloride	65.4
4	5	isopropyl alcohol	45.2
5	5	Toluene	47.8
6	5	n–hexane	45.2
7	2	methanol	70.1
8	7.5	methanol	98.5

Table S6 Comparison of the catalytic activity of various materials for nitrobenzene reduction

Entry	Catalyst	Light source	t	T(℃)	Yield(%)	TON/TOF(h^{-1})	Ref
1	$\{PW_{11}O_{39}\}$	10 W LED lamp	6 h	RT	99.8	350/58	This
2	{Ag6}	10 W 365 nm LED lamp	2.5 h	RT	98.55	1061.9/424.8	[3]
3	$\{Te_2W_{20}O_{72}\}$	10 W LED lamp	6 h	RT	99.8	330/24	[4]
4	Rh-$\{As_4W_{40}\}$	10 W LED lamp	6 h	RT	96.2	-/-	[5]
5	{ZnW-TPT}	10 W 365 nm LED lamp	6 h	RT	>99	208/-	[6]
6	1-Sb_8Mo_{18}	-	2 h	80℃	100	-/-	[7]
7	Ru-WO_6	10 W 365 nm LED lamp	6 h	RT	97	-/-	[8]
8	$Mo^{IV}{}_3$ $\{O_8Mo_4\}_3$	-	2 h	80℃	100	-/-	[9]
9	g-C_3N_4	300 W Xe lamp (λ > 42 nm)	1 h	RT	83	-/-	[10]
10	Pt/SWO-NS	Visible light (λ ≥ 420)	2 h	RT	>99	-/-	[11]
11	rGO/Cu_2O-CuO-3	(30 W-LED, λ > 420 nm)	45 min	25℃	100	-/-	[12]
12	$Bi_2W_{1-x}Mo_xO_6$	visible light (λ ≥ 420 nm)	30 min	RT	98	-/-	[13]

Supplementary figures for structure and characterization

Figure S1. Image of the photocatalytic reactor

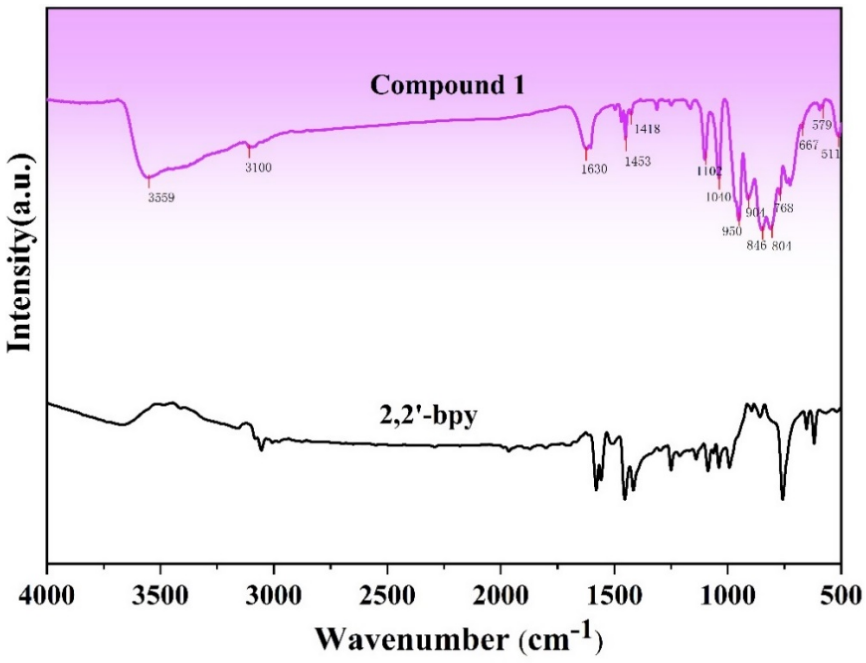

Figure S2 FT-IR spectrum of compound **1** and and 2,2'-bipyridine

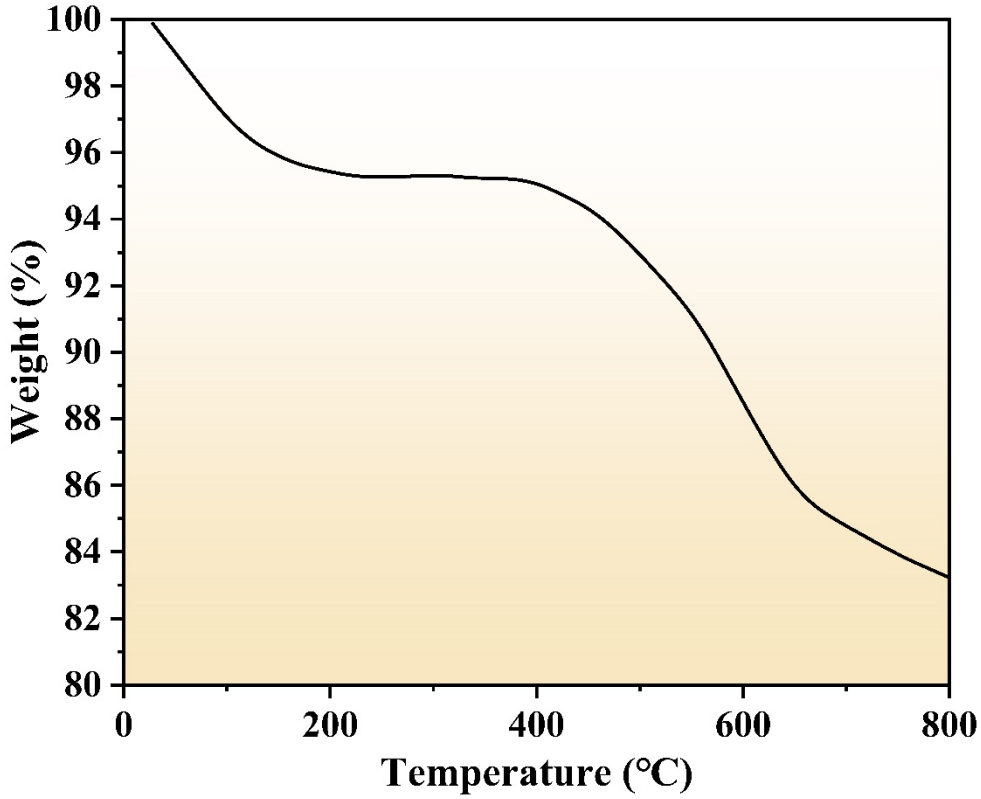

Figure S3 TGA curve of **1**

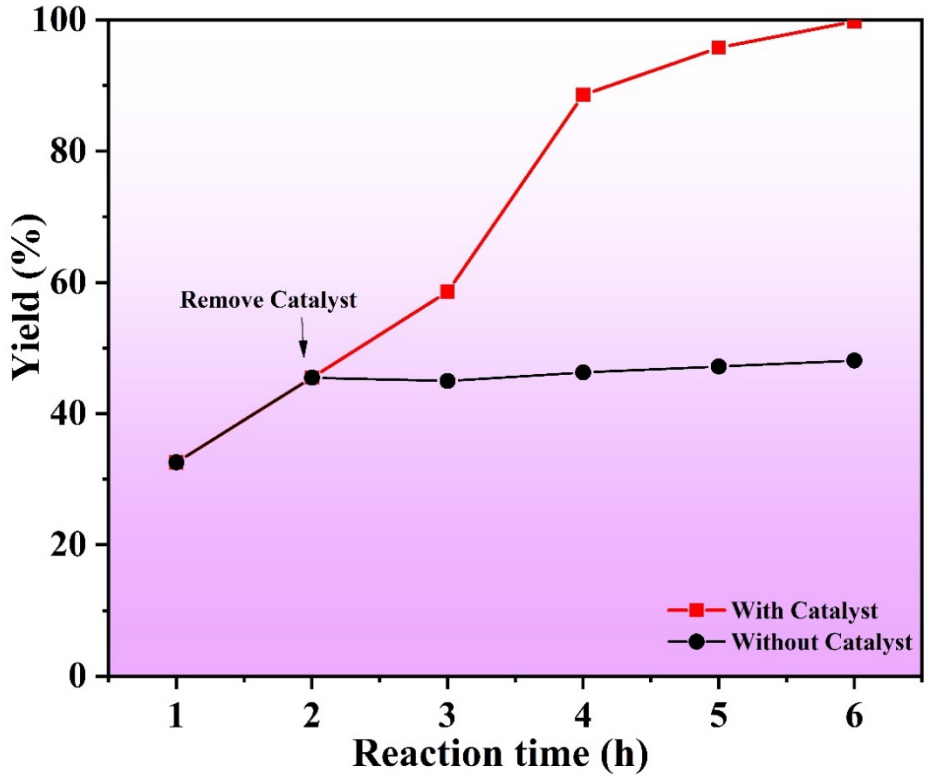

Figure S4 Hot filtration test of **1**

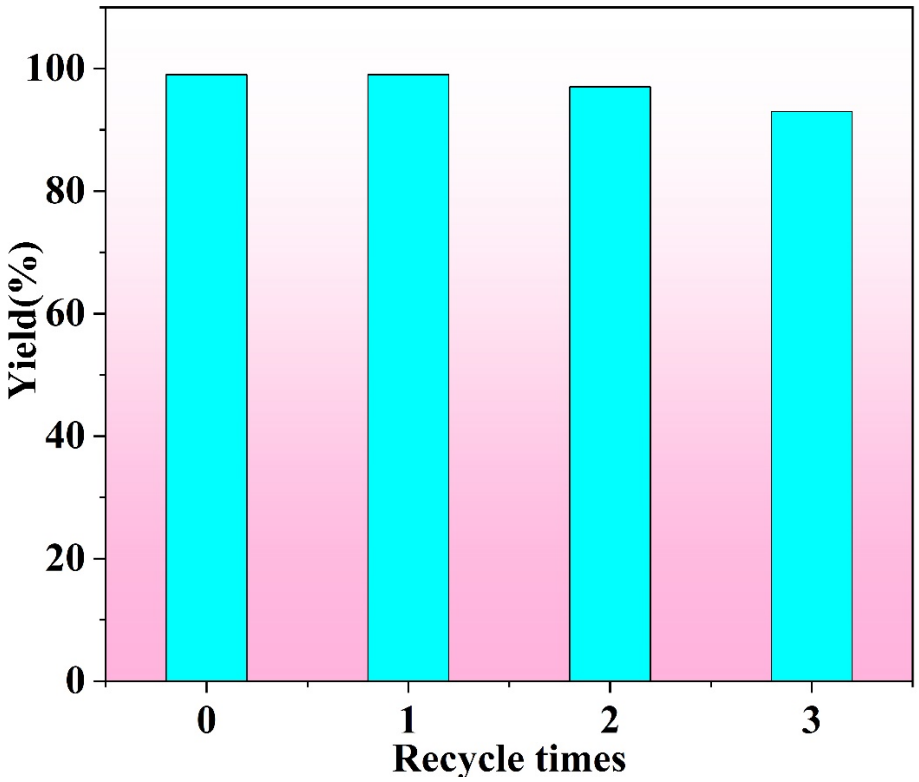

Figure S5 Recycling experiment for the reduction of nitrobenzene

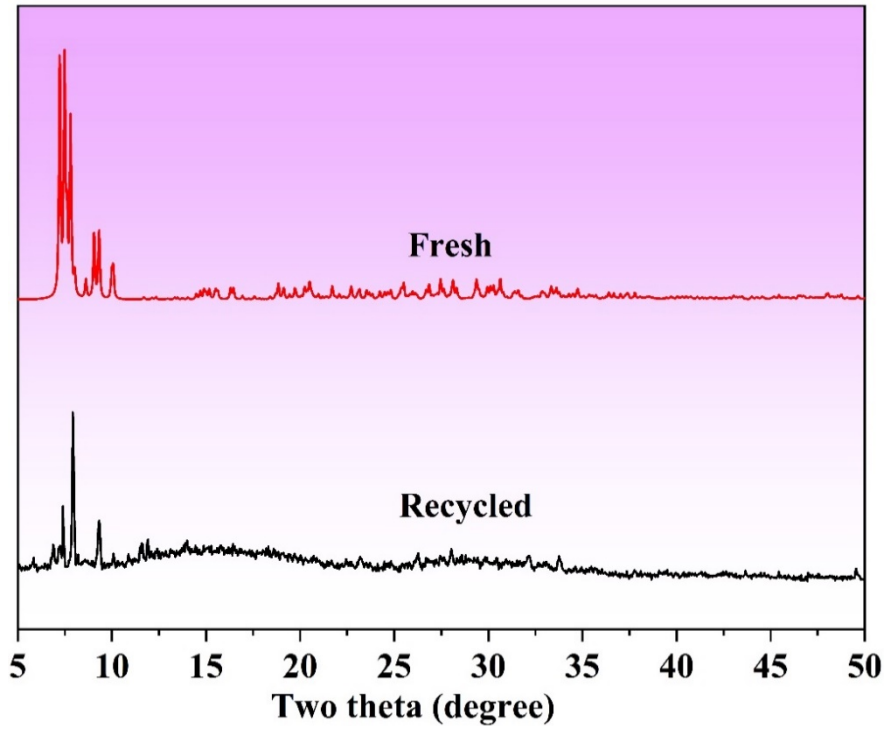

Figure S6 PXRD patterns of **1** before and after the photocatalytic reaction

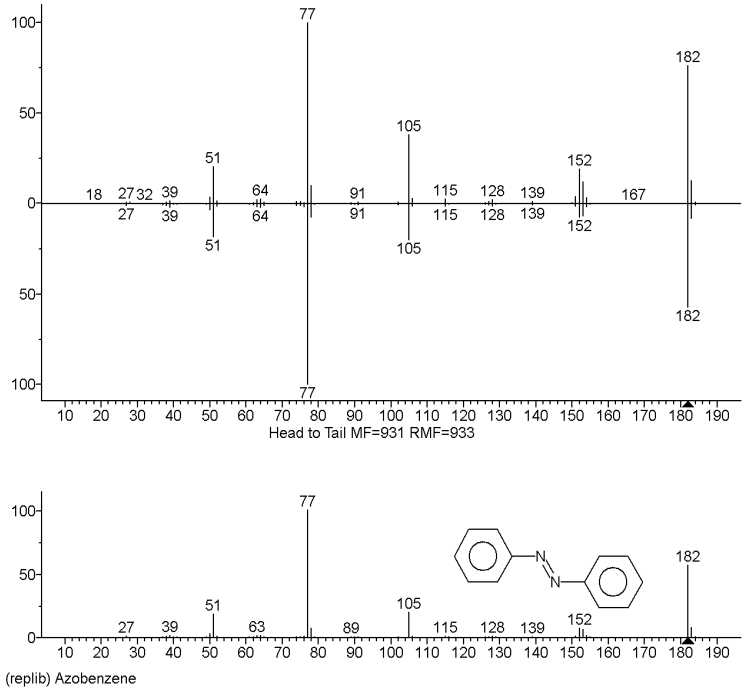

Figure S7. The GC–MS spectrum of intermediate azobenzene (bottom, simulation; top, experiment)

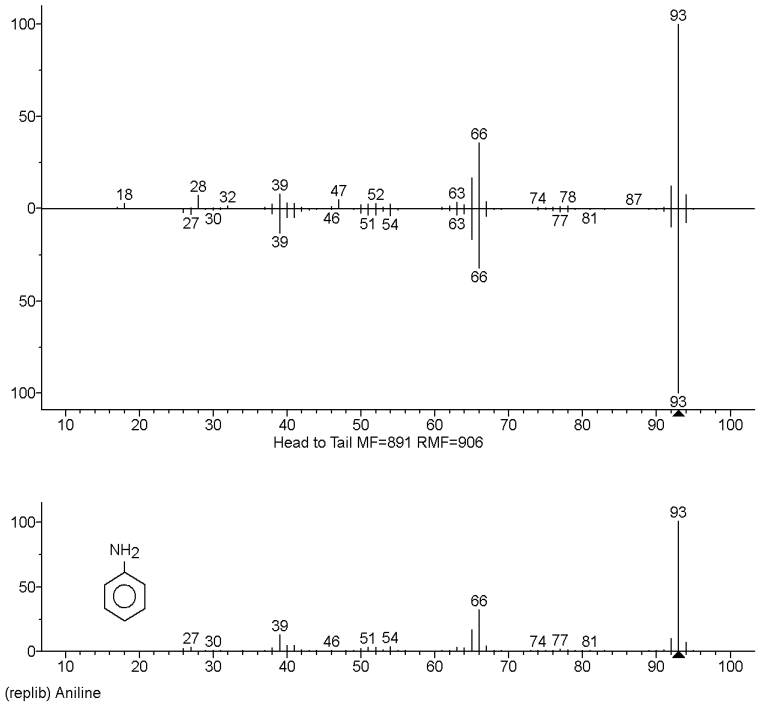

Figure S8 The GC–MS spectrum of aniline (bottom, simulation; top, experiment)

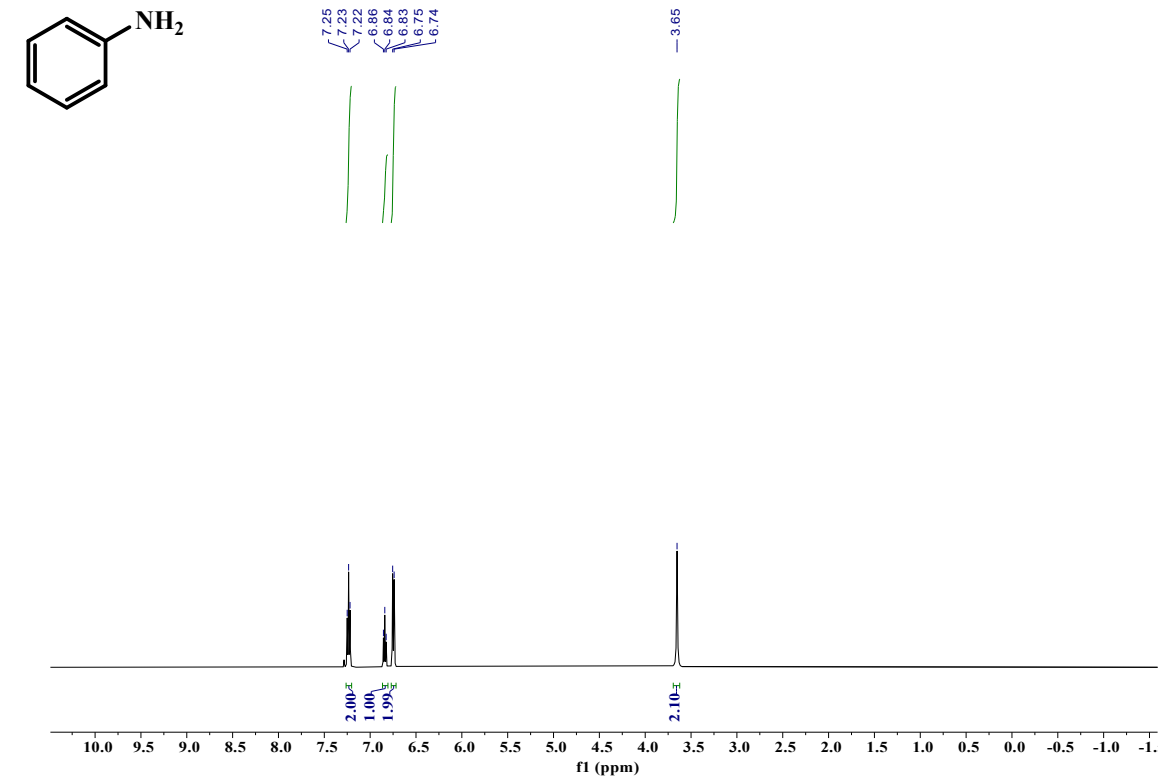

Figure. S9 ^{1}H NMR spectra of 2a (500 MHz, $CDCl_3$)

Aniline(2a): ^{1}H NMR (500 MHz, Chloroform–*d*) δ 7.23 (t, *J* = 7.7 Hz, 2H), 6.84 (t, *J* = 7.4 Hz, 1H), 6.75 (d, *J* = 7.9 Hz, 2H), 3.65 (s, 2H).

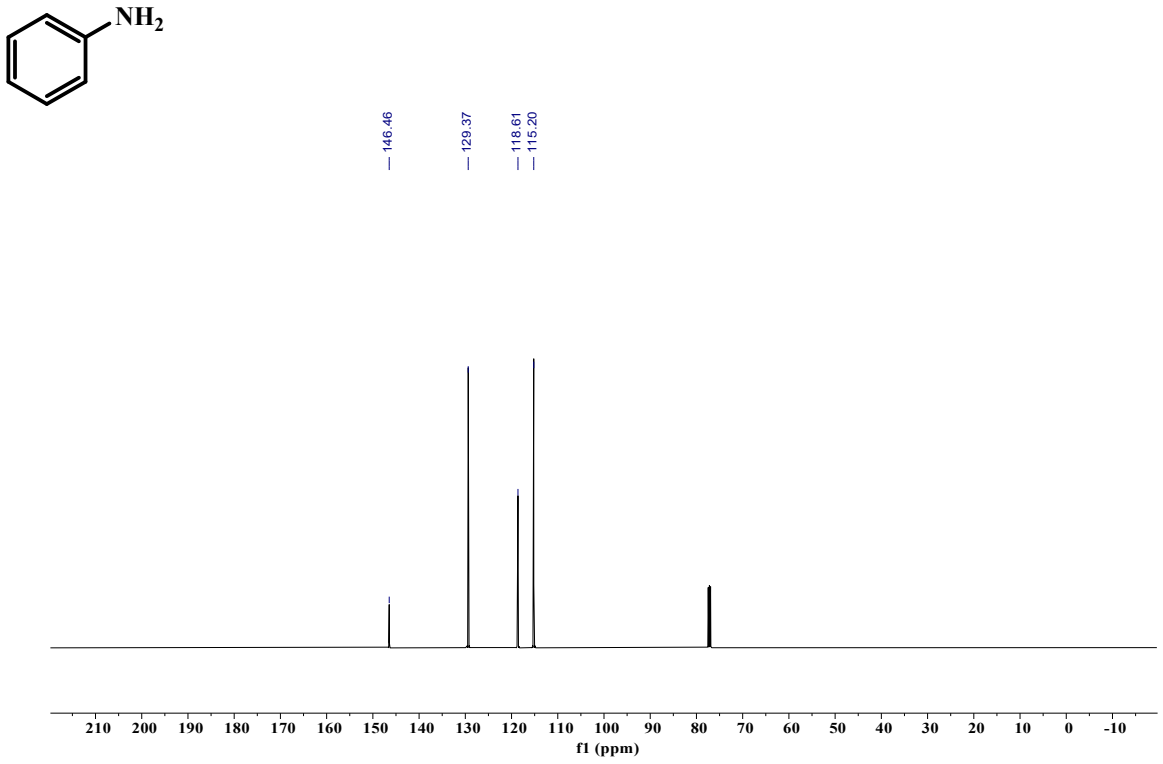

Figure. S10 ^{13}C NMR spectra of 2a (126 MHz, $CDCl_3$).

Aniline(2a): ^{13}C NMR (126 MHz, Chloroform–d) δ 146.46(s), 129.37(s), 118.61(s), 115.20(s).

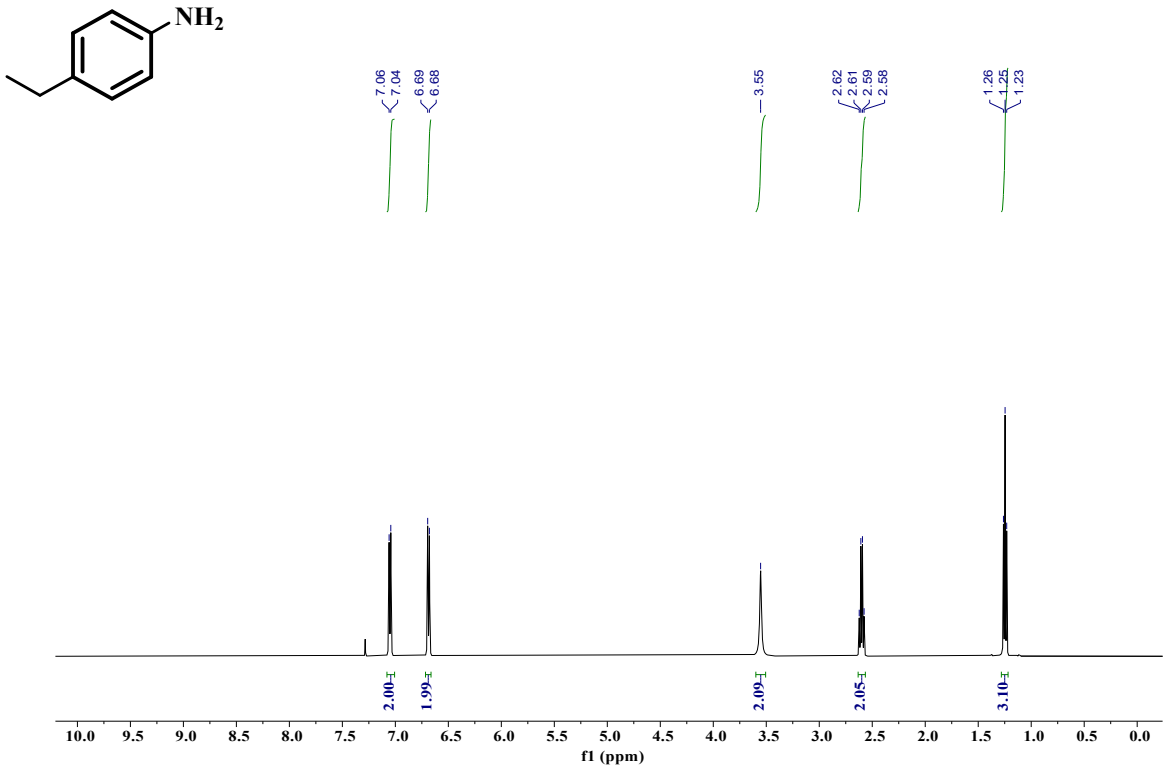

Figure. S11 ^{1}H NMR spectra of 2b (500 MHz, $CDCl_3$)
4–Ethylaniline (2b): ^{1}H NMR (500 MHz, Chloroform–d) δ 7.05 (d, J = 8.0 Hz, 2H), 6.69 (d, J = 8.1 Hz, 2H), 3.55 (s, 2H), 2.60 (q, J = 7.6 Hz, 2H), 1.25 (t, J = 7.6 Hz, 3H).

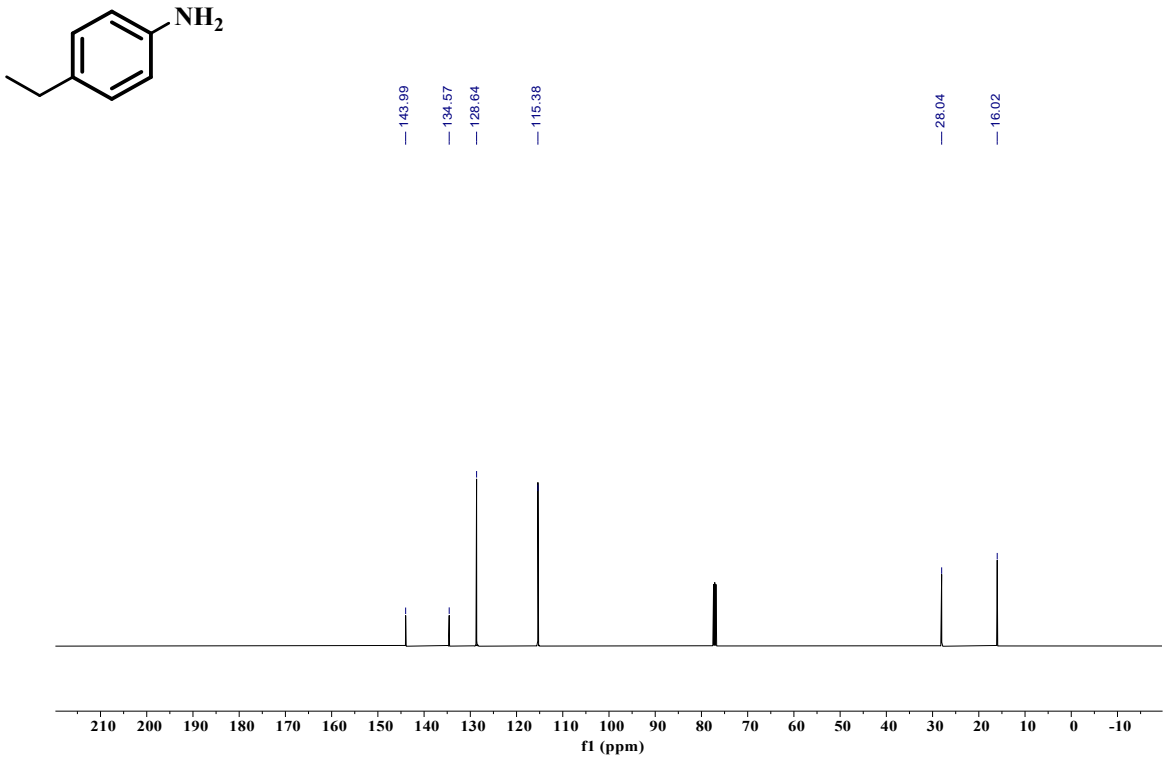

Figure. S12 ^{13}C NMR spectra of 2e (126 MHz, $CDCl_3$).
4–Ethylaniline (2b):^{13}C NMR (126 MHz, Chloroform–d) δ 143.99(s), 134.57(s), 128.64(s), 115.38(s), 28.04(s), 16.02(s).

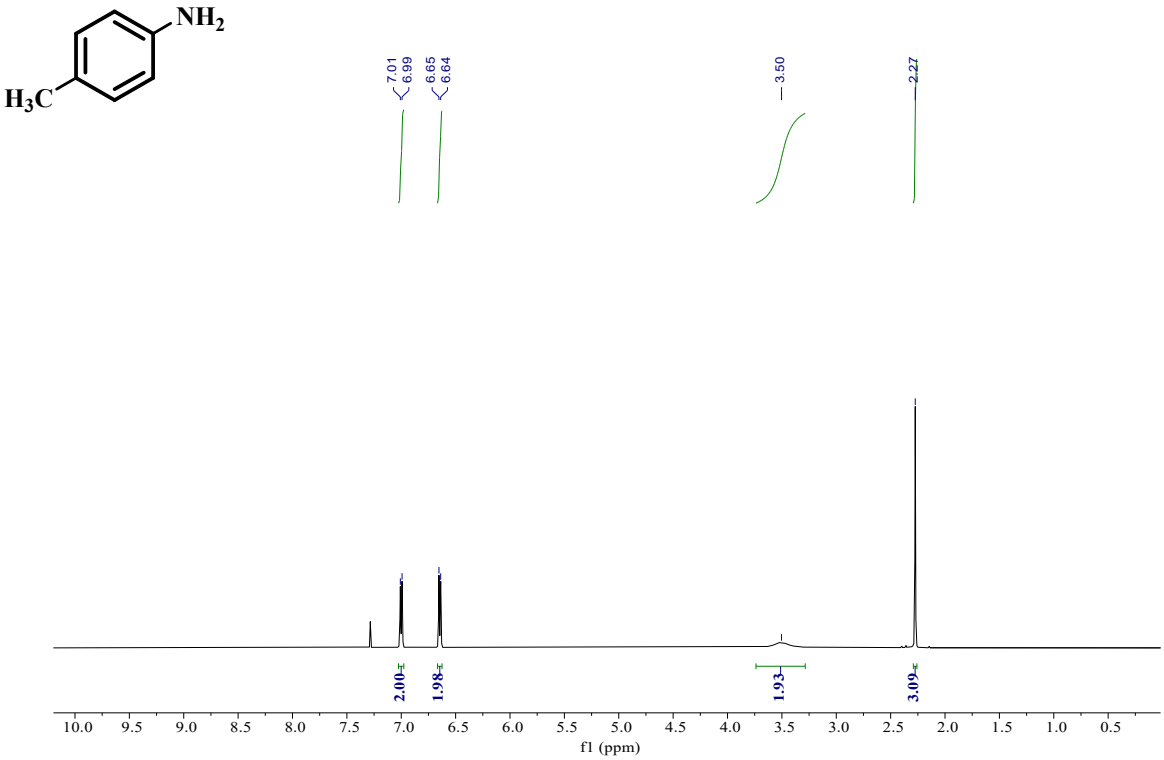

Figure. S13 ^{1}H NMR spectra of 2b (500 MHz, $CDCl_3$).
p–Toluidine (2c): ^{1}H NMR (500 MHz, Chloroform–d) δ 7.00 (d, J = 7.9 Hz, 2H), 6.65 (d, J = 8.0 Hz, 2H), 3.50 (s, 2H), 2.27 (s, 3H).

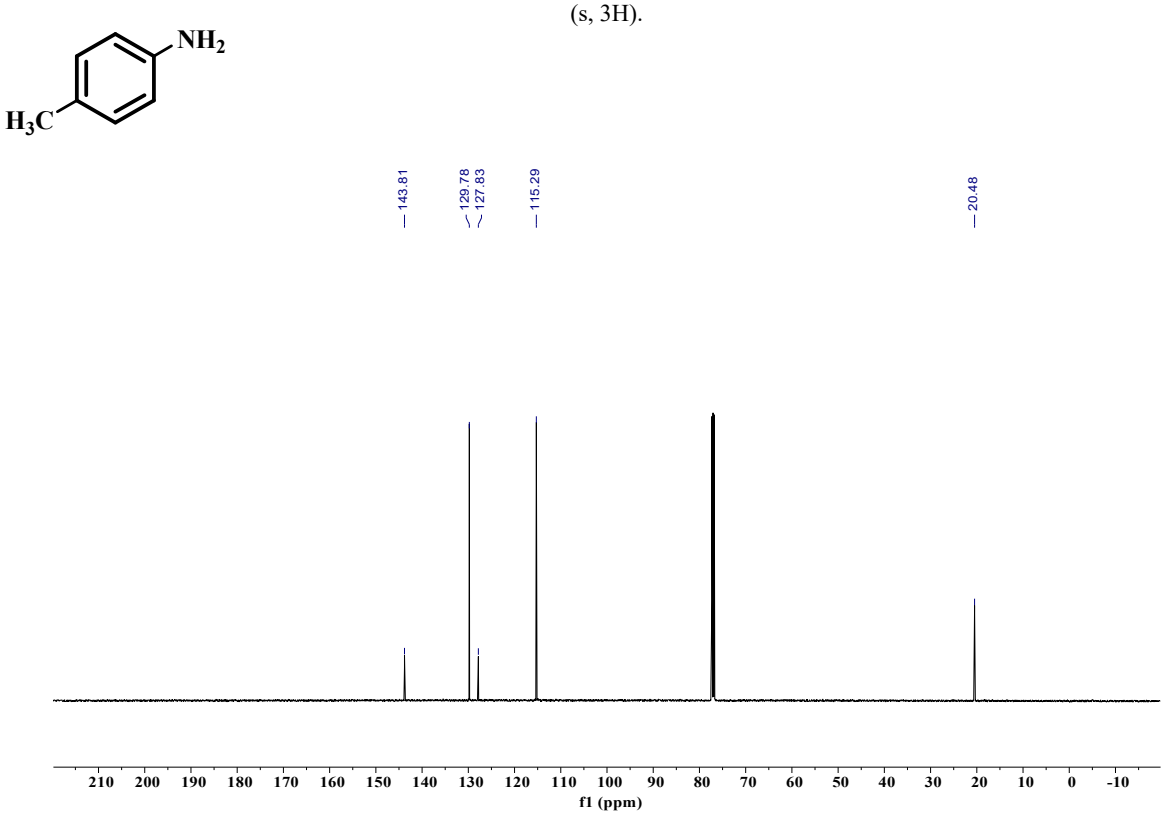

Figure. S14 ^{13}C NMR spectra of 2b (126 MHz, $CDCl_3$)
p–Toluidine (2c): ^{13}C NMR (126 MHz, Chloroform–d) δ 143.81(s), 129.78(s), 127.83(s), 115.29(s), 20.48(s).

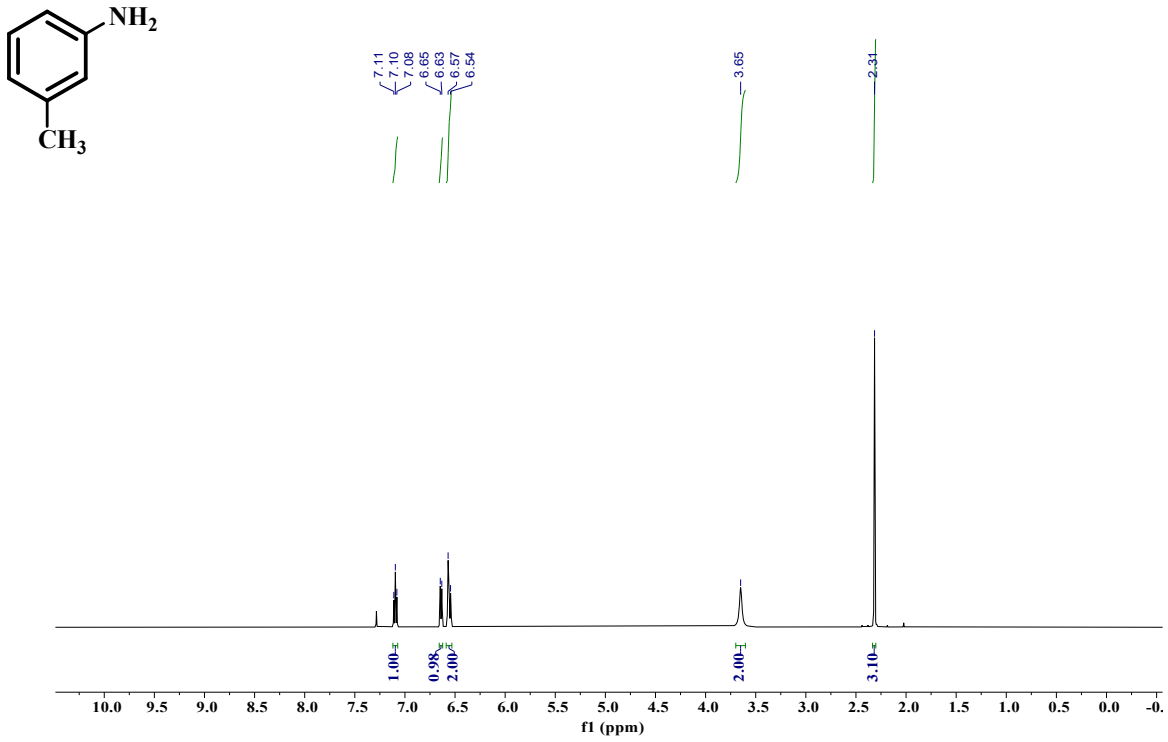

Figure. S15 ^{1}H NMR spectra of 2c (500 MHz, $CDCl_3$).
m–Toluidine (2d): ^{1}H NMR (500 MHz, Chloroform–d) δ 7.10 (t, J = 7.6 Hz, 1H), 6.64 (d, J = 7.5 Hz, 1H), 6.56 (d, J = 12.2 Hz, 2H), 3.65 (s, 2H), 2.31 (s, 3H).

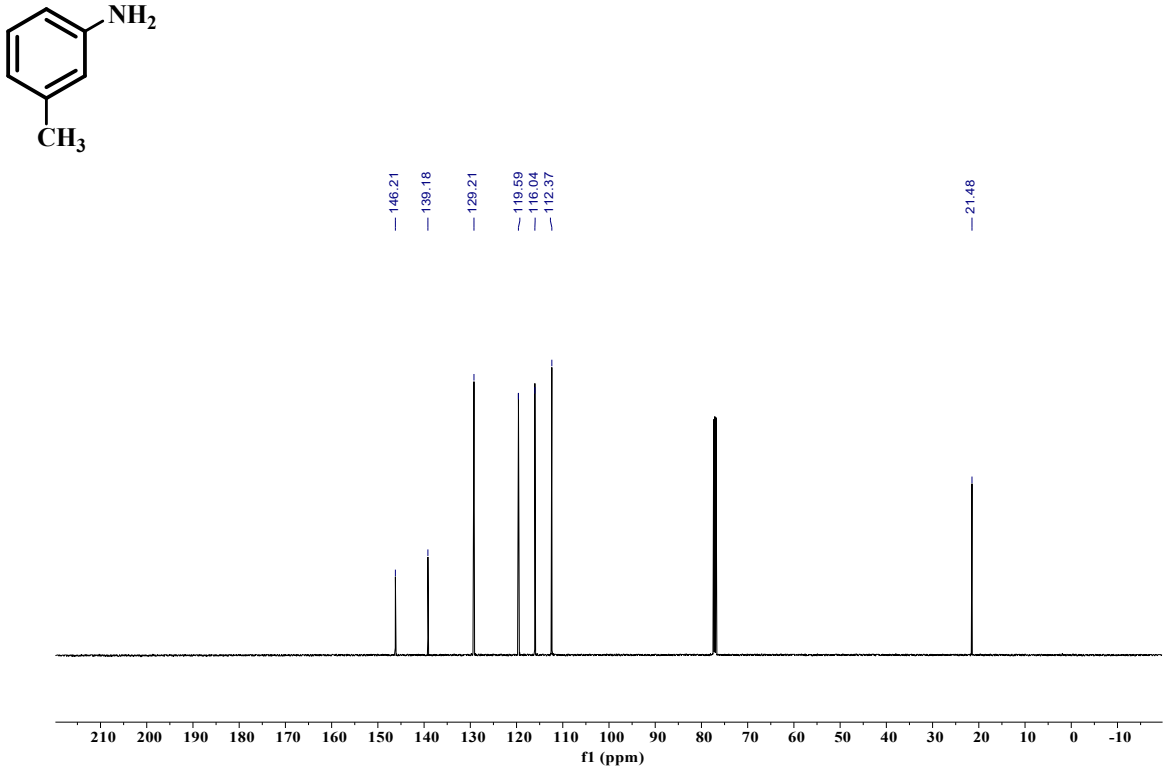

Figure. S16 ^{13}C NMR spectra of 2c (126 MHz, $CDCl_3$).
m–Toluidine (2d): ^{13}C NMR (126 MHz, Chloroform–d) δ 146.21(s), 139.18(s), 129.21(s), 119.59(s), 116.04(s), 112.37(s), 21.48(s).

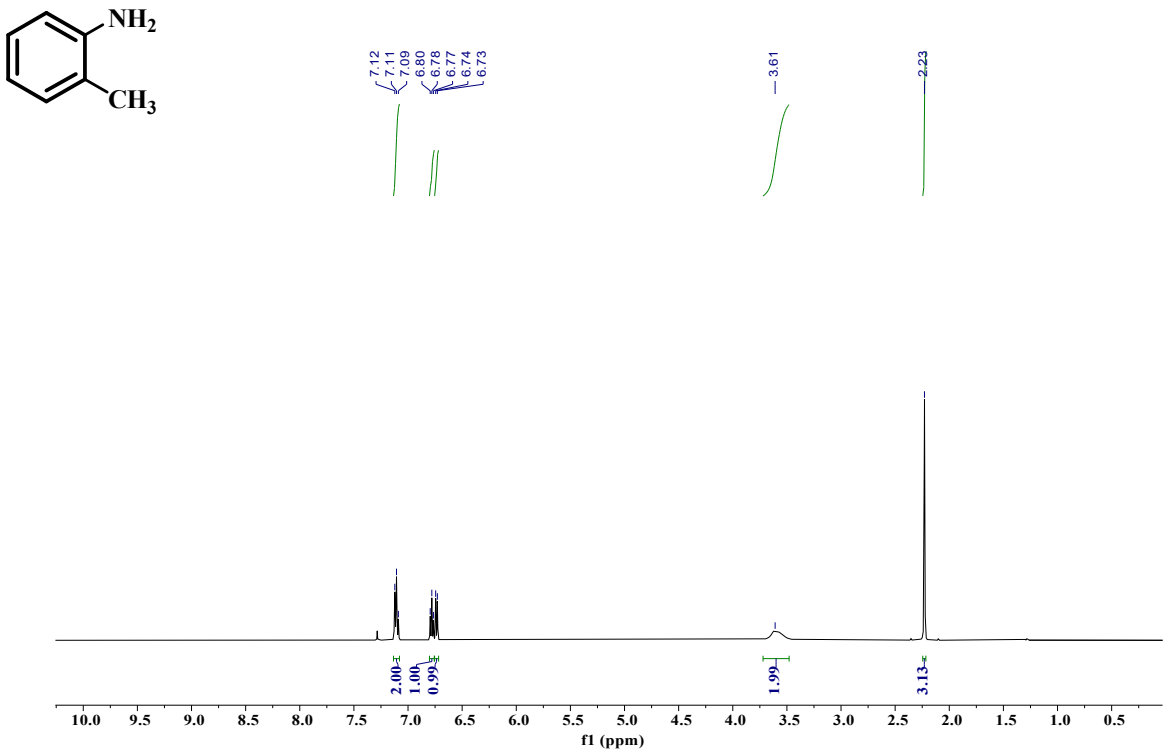

Figure. S17 ^{1}H NMR spectra of 2d (500 MHz, $CDCl_3$).

o–Toluidine (2e): ^{1}H NMR (500 MHz, Chloroform–d) δ 7.11 (t, J = 8.3 Hz, 2H), 6.78 (t, J = 7.4 Hz, 1H), 6.74 (d, J = 7.8 Hz, 1H), 3.61 (s, 2H), 2.23 (s, 3H).

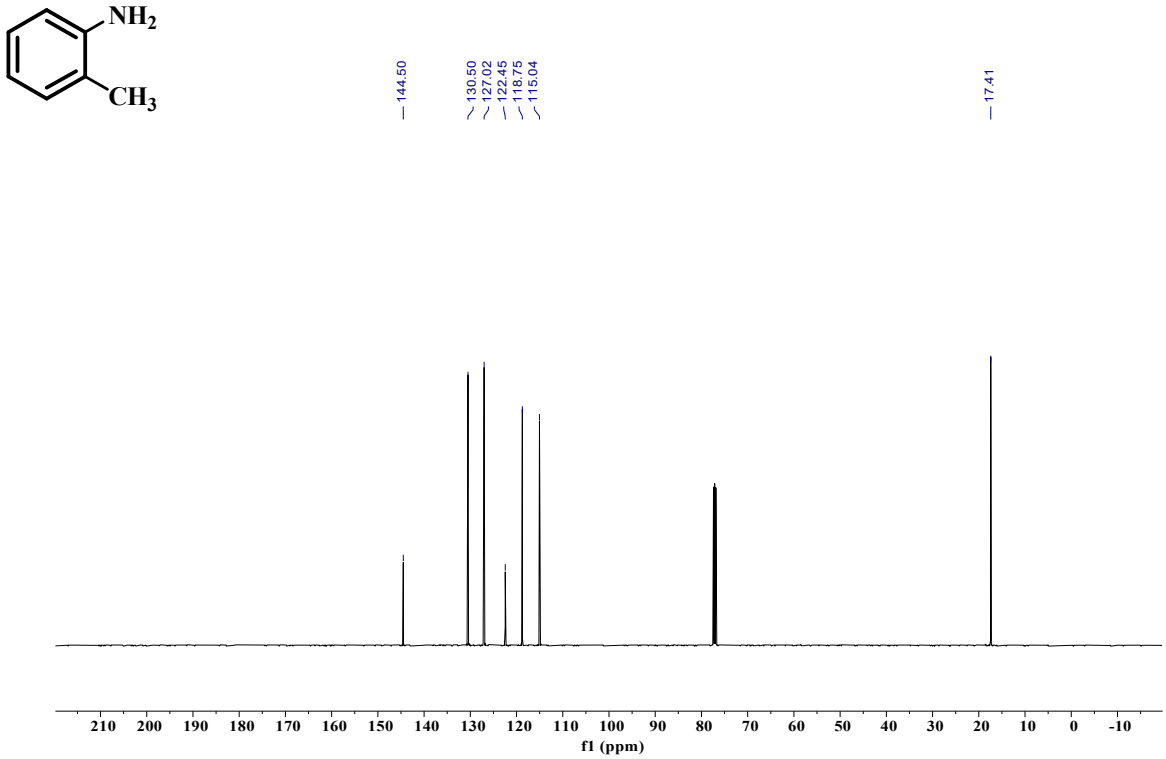

Figure. S18 ^{13}C NMR spectra of 2d (126 MHz, $CDCl_3$)

o–Toluidine (2e): ^{13}C NMR (126 MHz, Chloroform–*d*) δ 144.50(s), 130.50(s), 127.02(s), 122.45(s), 118.75(s), 115.04(s), 17.41(s).

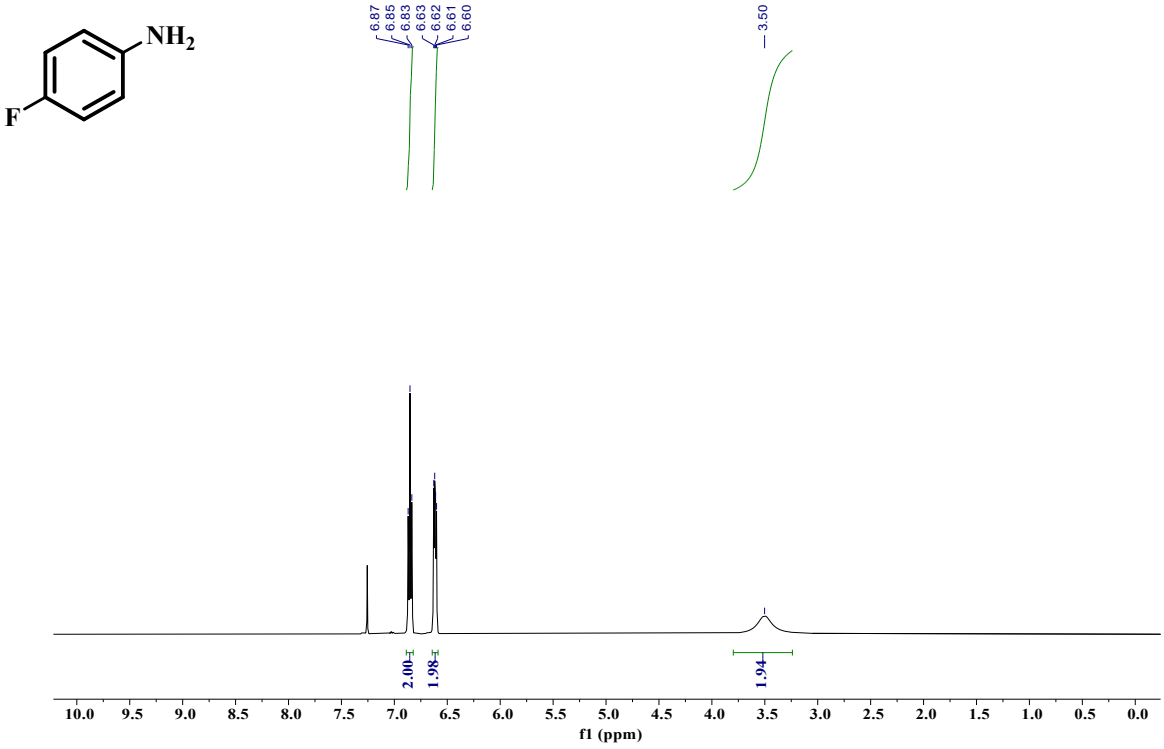

Figure. S19 ^{1}H NMR spectra of 2g (500 MHz, $CDCl_3$).
4–Fluoroaniline (2f): ^{1}H NMR (500 MHz, Chloroform–d) δ 6.85 (t, J = 8.7 Hz, 2H), 6.61 (dd, J = 8.7, 4.5 Hz, 2H), 3.50 (s, 2H).

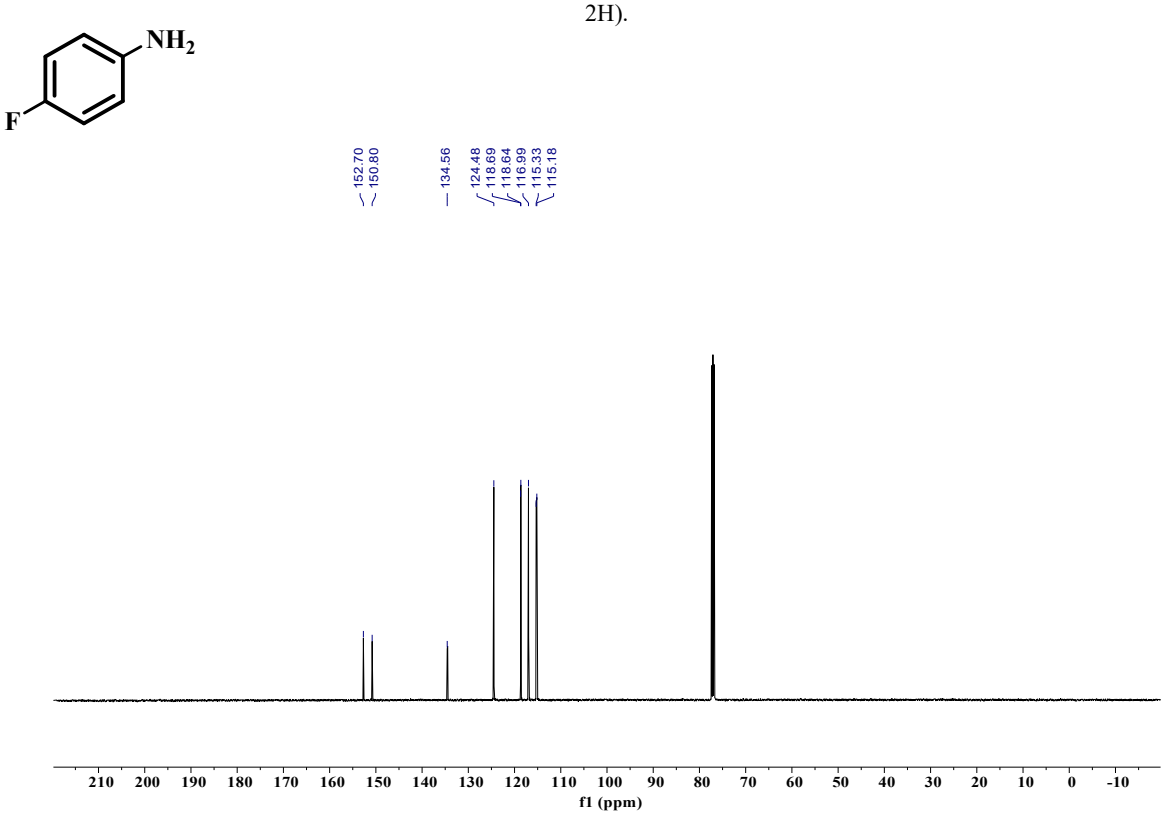

Figure. S20 ^{13}C NMR spectra of 2g (126 MHz, $CDCl_3$).
4–Fluoroaniline (2f): ^{13}C NMR (126 MHz, Chloroform–d) δ 152.70(s), 150.80(s), 134.56(s), 124.48(s), 118.69(s), 118.64(s), 116.99(s), 115.33(s), 115.18(s).

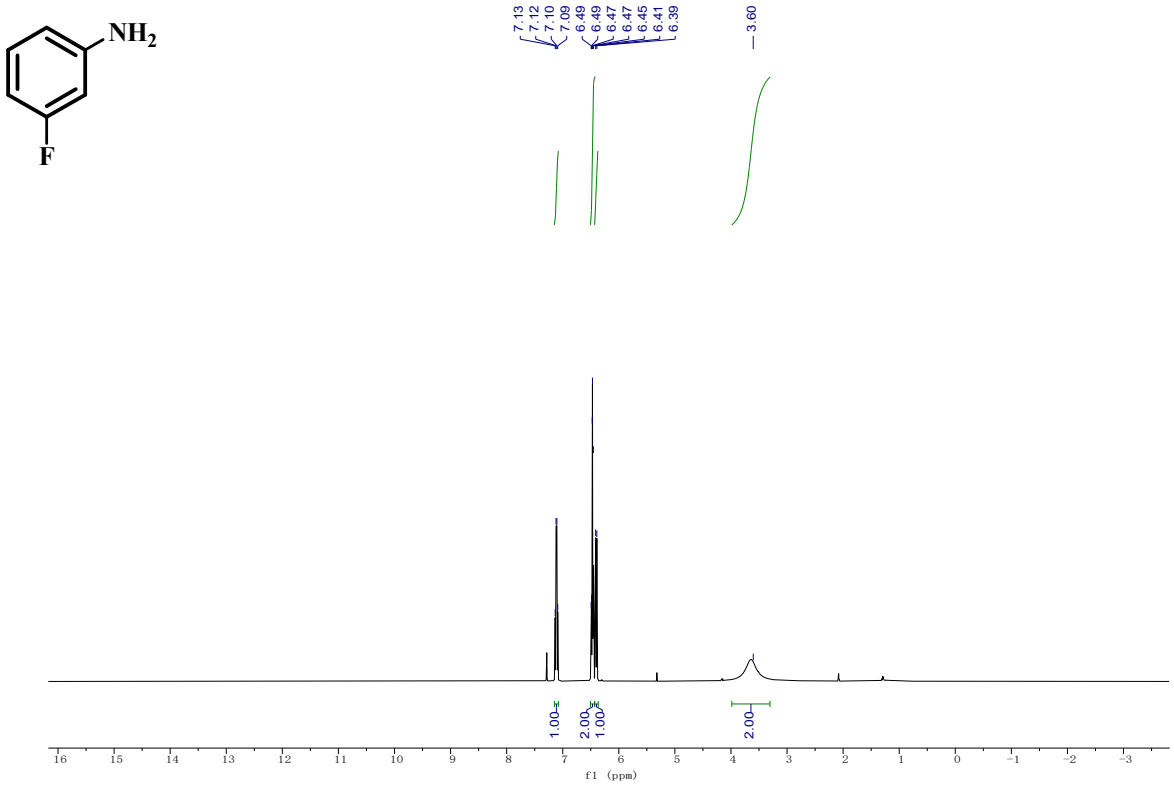

Figure. S21 ^{1}H NMR spectra of 2f (500 MHz, $CDCl_3$).
3–Fluoroaniline (2g): ^{1}H NMR (500 MHz, Chloroform–d) δ 7.11 (q, J = 7.7 Hz, 1H), 6.51 – 6.43 (m, 2H), 6.40 (d, J = 11.0 Hz, 1H), 3.60 (s, 2H).

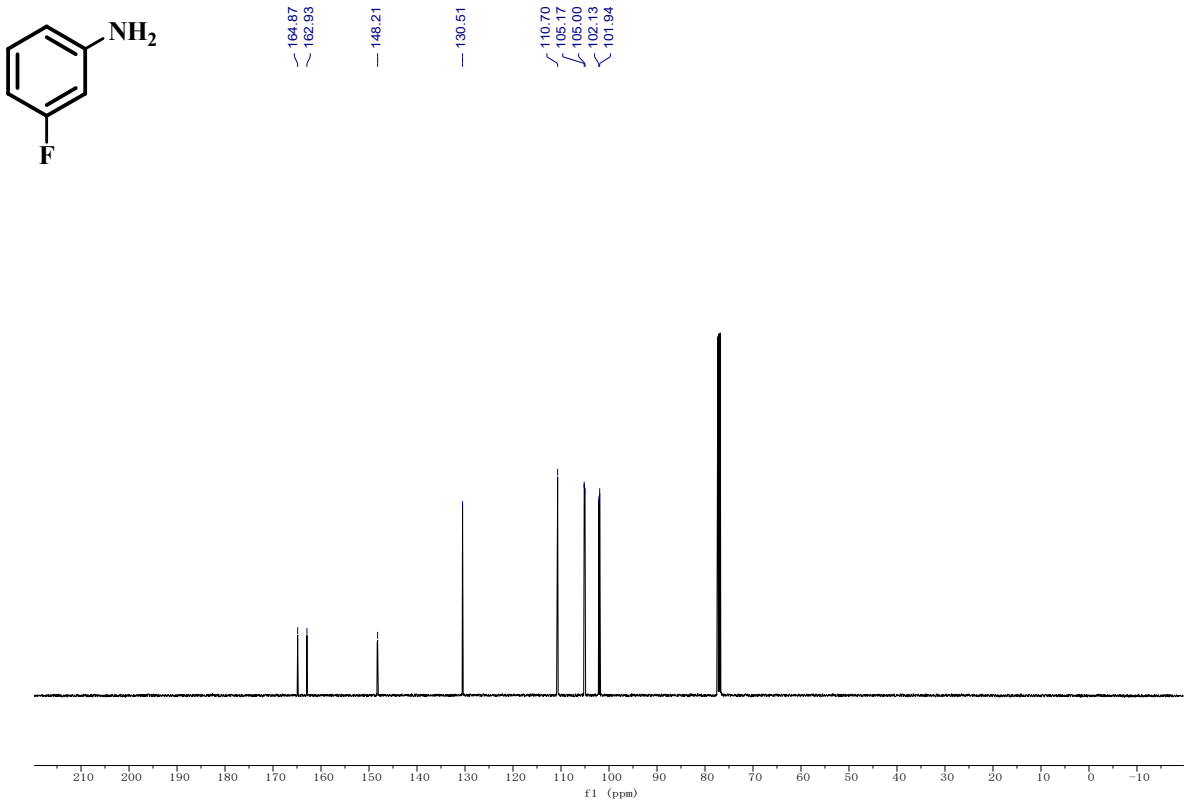

Figure. S22 ^{13}C NMR spectra of 2f (126 MHz, $CDCl_3$).
3–Fluoroaniline (2g): ^{13}C NMR (126 MHz, Chloroform–d) δ 164.87(s), 162.93(s), 148.21(s), 130.51(s), 110.70(s), 105.17(s), 105.00(s), 102.13(s), 101.94(s).

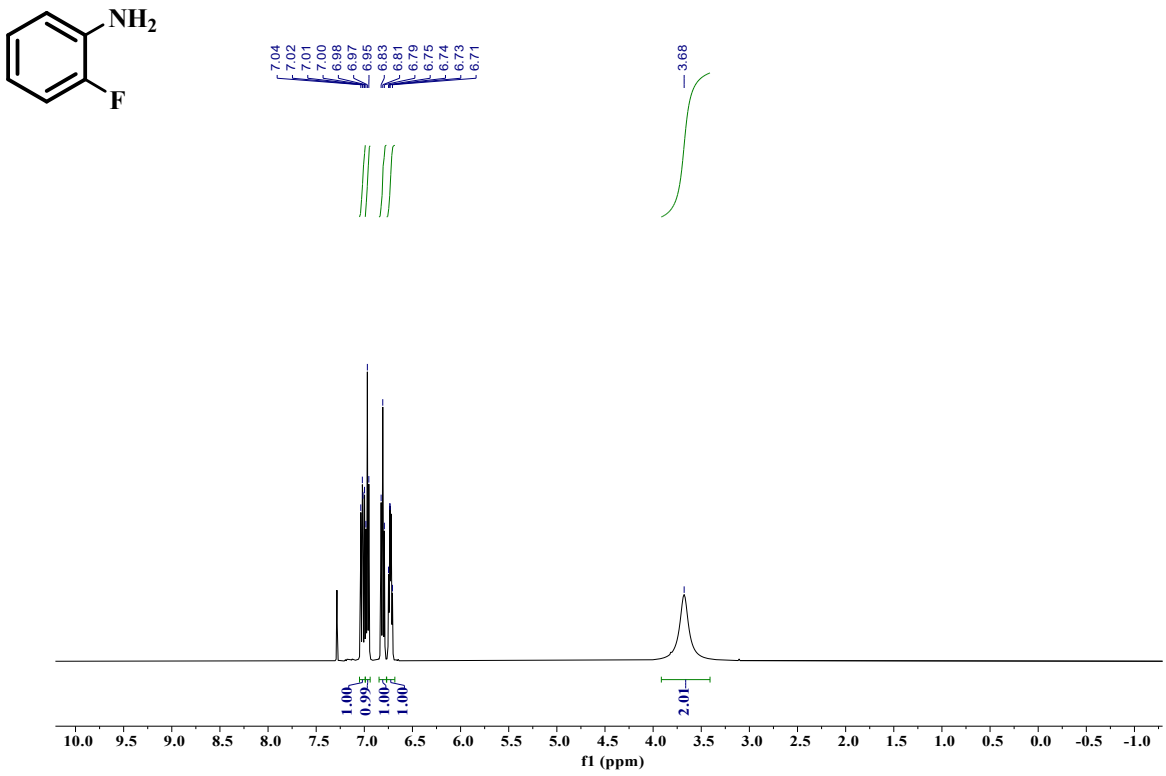

Figure. S23 ^{1}H NMR spectra of 2g (500 MHz, $CDCl_3$).
2–Fluoroaniline(2h): ^{1}H NMR (500 MHz, Chloroform–d) δ 7.02 (dd, J = 11.4, 8.1 Hz, 1H), 6.97 (t, J = 7.7 Hz, 1H), 6.81 (t, J = 8.4 Hz, 1H), 6.77 – 6.68 (m, 1H), 3.68 (s, 2H).

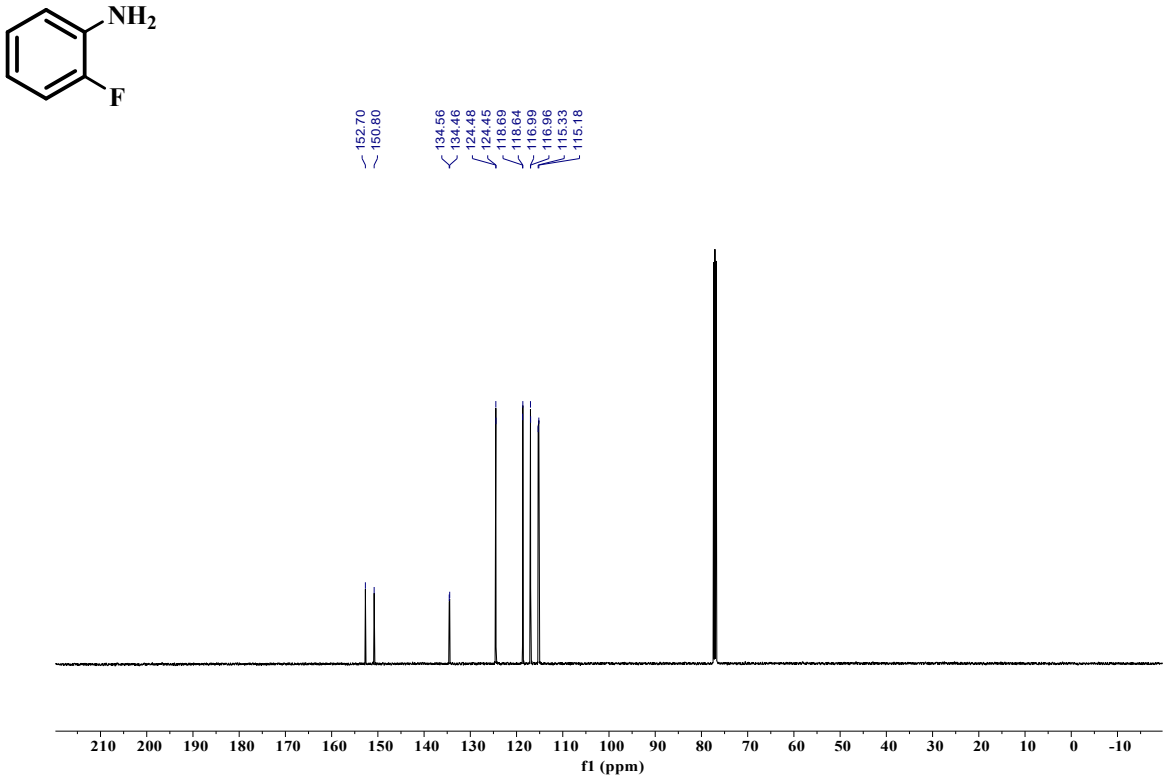

Figure. S24 ^{13}C NMR spectra of 2g (126 MHz, $CDCl_3$).
2–Fluoroaniline(2h): ^{13}C NMR (126 MHz, Chloroform–d) δ 152.70(s), 150.80(s), 134.56(s), 134.46(s), 124.48(s), 124.45(s), 118.69(s), 118.64(s), 116.99(s), 116.96(s), 115.33(s), 115.18(s).

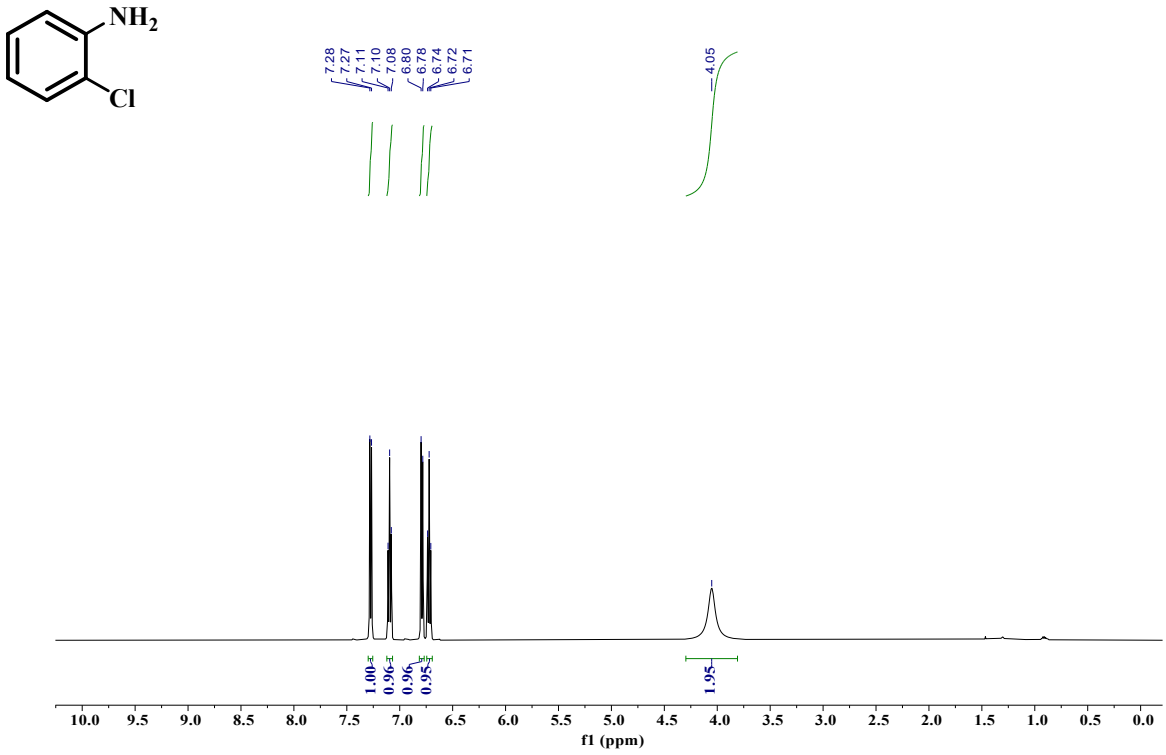

Figure. S25 ^{1}H NMR spectra of 2h (500 MHz, $CDCl_3$).

2–Chloroaniline (2i): ^{1}H NMR (500 MHz, Chloroform–d) δ 7.27 (d, J = 7.9 Hz, 1H), 7.10 (t, J = 7.7 Hz, 1H), 6.79 (d, J = 8.0 Hz, 1H), 6.72 (t, J = 7.6 Hz, 1H), 4.05 (s, 2H).

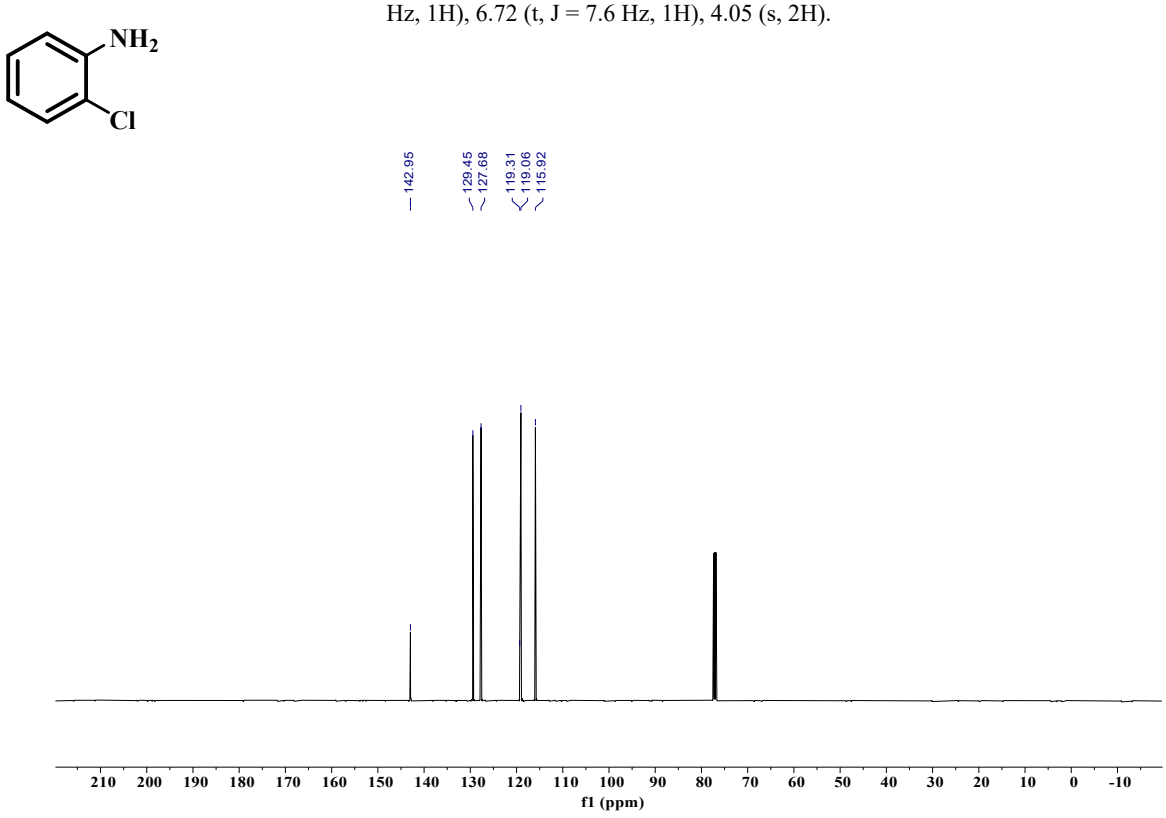

Figure. S26 ^{13}C NMR spectra of 2h (126 MHz, $CDCl_3$).

2–Chloroaniline (2i): ^{13}C NMR (126 MHz, Chloroform–d) δ 142.95(s), 129.45(s), 127.68(s), 119.31(s), 119.06(s), 115.92(s).

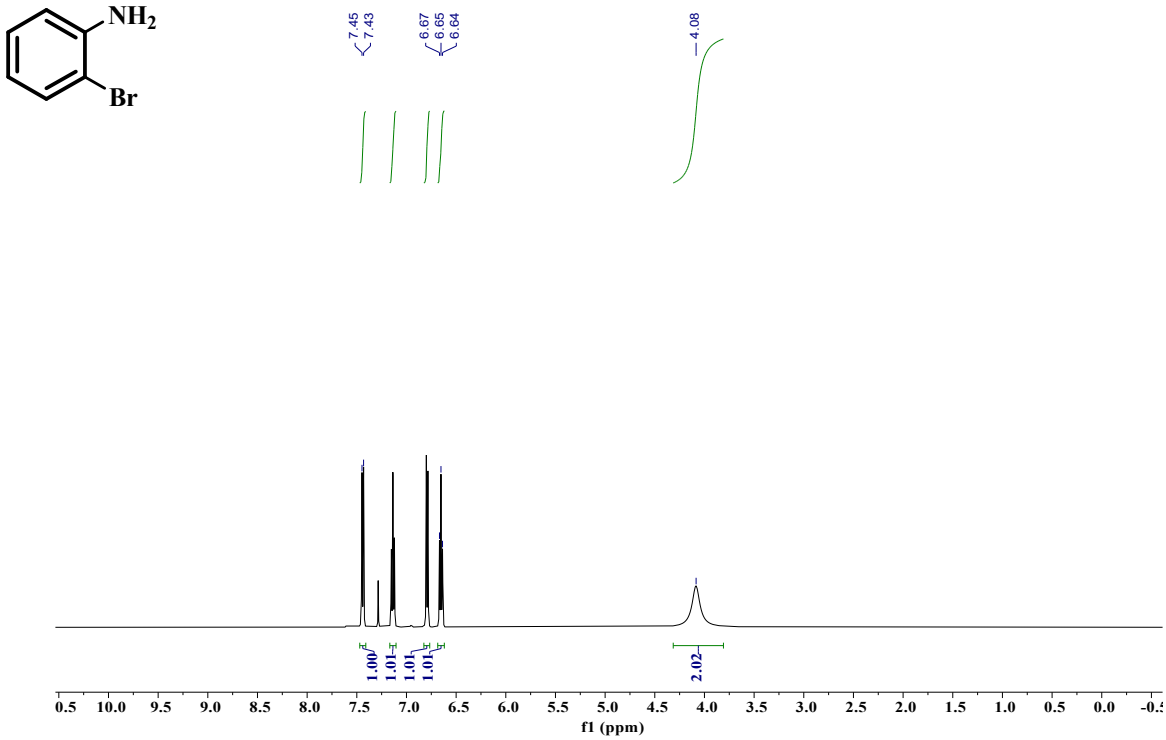

Figure. S27 ^{1}H NMR spectra of 2i (500 MHz, $CDCl_3$).
2–Bromoaniline (2j): ^{1}H NMR (500 MHz, Chloroform–d) δ 7.44 (d, J = 8.0 Hz, 1H), 7.17 – 7.11 (m, 1H), 6.79 (dt, J = 8.0, 1.5 Hz, 1H), 6.65 (t, J = 7.6 Hz, 1H), 4.08 (s, 2H).

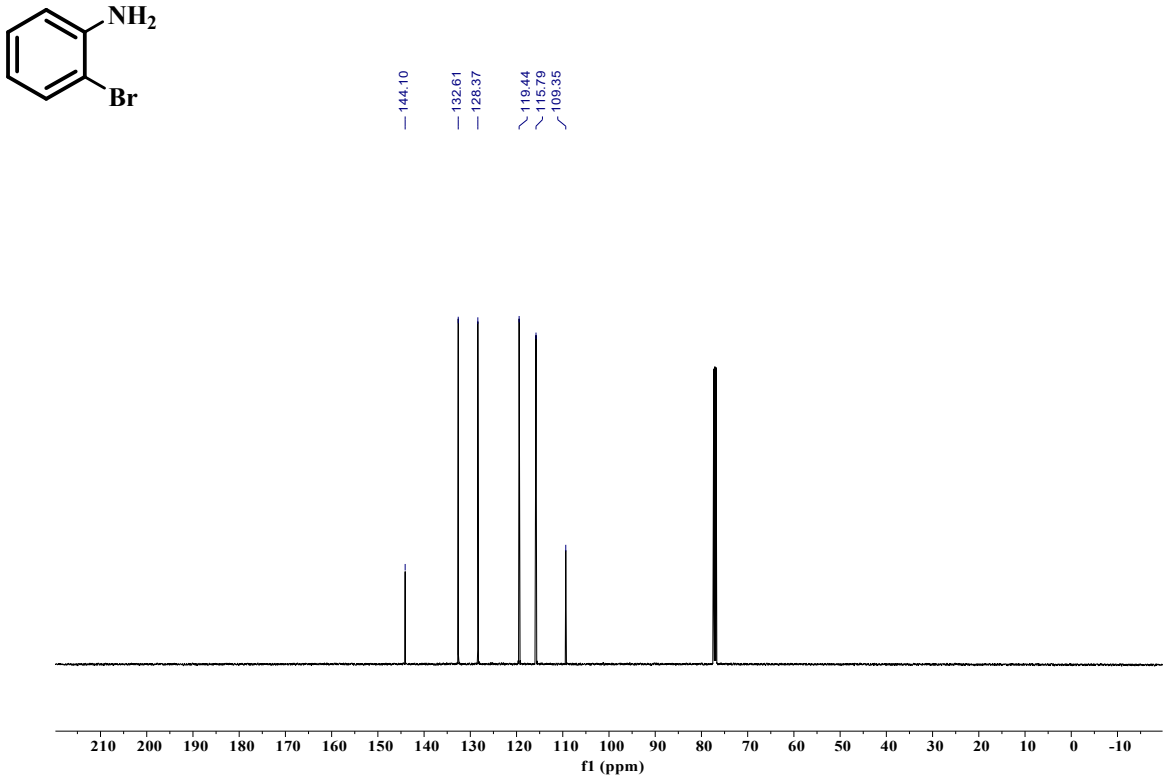

Figure. S28 ^{13}C NMR spectra of 2i (126 MHz, $CDCl_3$).
2–Bromoaniline (2j): ^{13}C NMR (126 MHz, Chloroform–d) δ 144.10(s), 132.61(s), 128.37(s), 119.44(s), 115.79(s), 109.35(s).

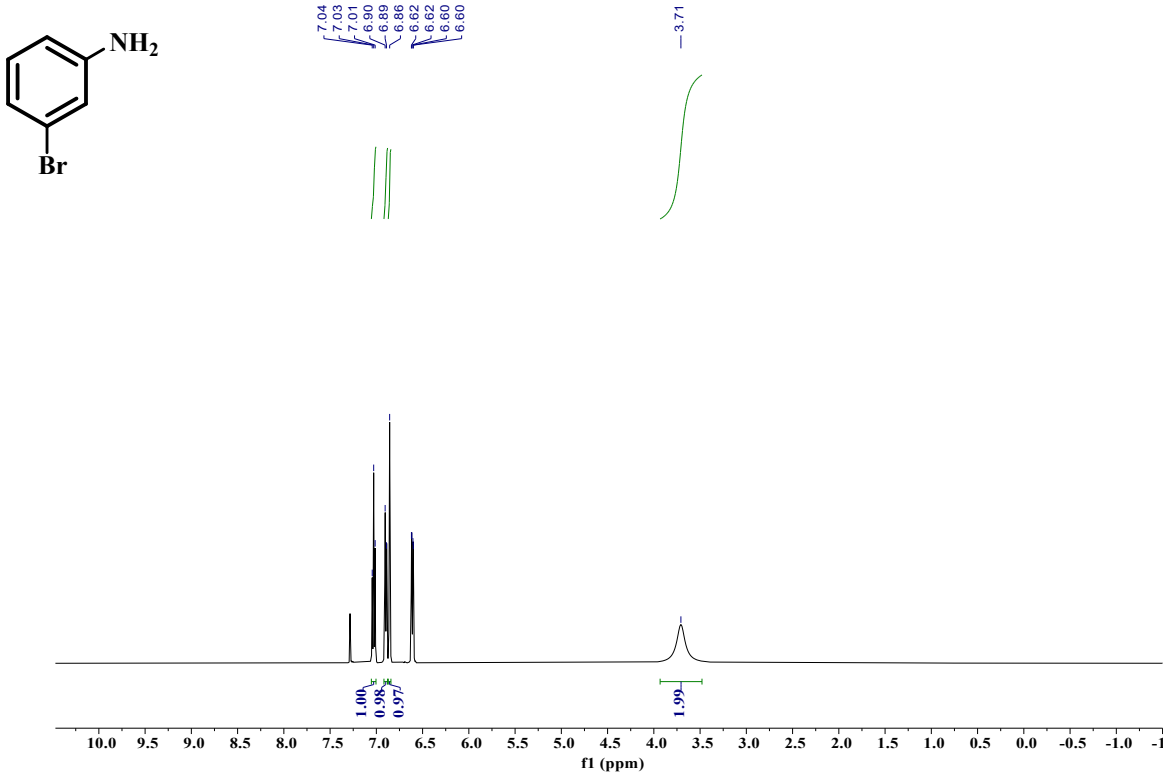

Figure. S29 ^{1}H NMR spectra of 2i (500 MHz, $CDCl_3$).
3–Bromoaniline (2k): ^{1}H NMR (500 MHz, Chloroform–d) δ 7.03 (t, J = 7.9 Hz, 1H), 6.90 (d, J = 7.3 Hz, 1H), 6.86 (s, 1H), 3.71 (s, 2H).

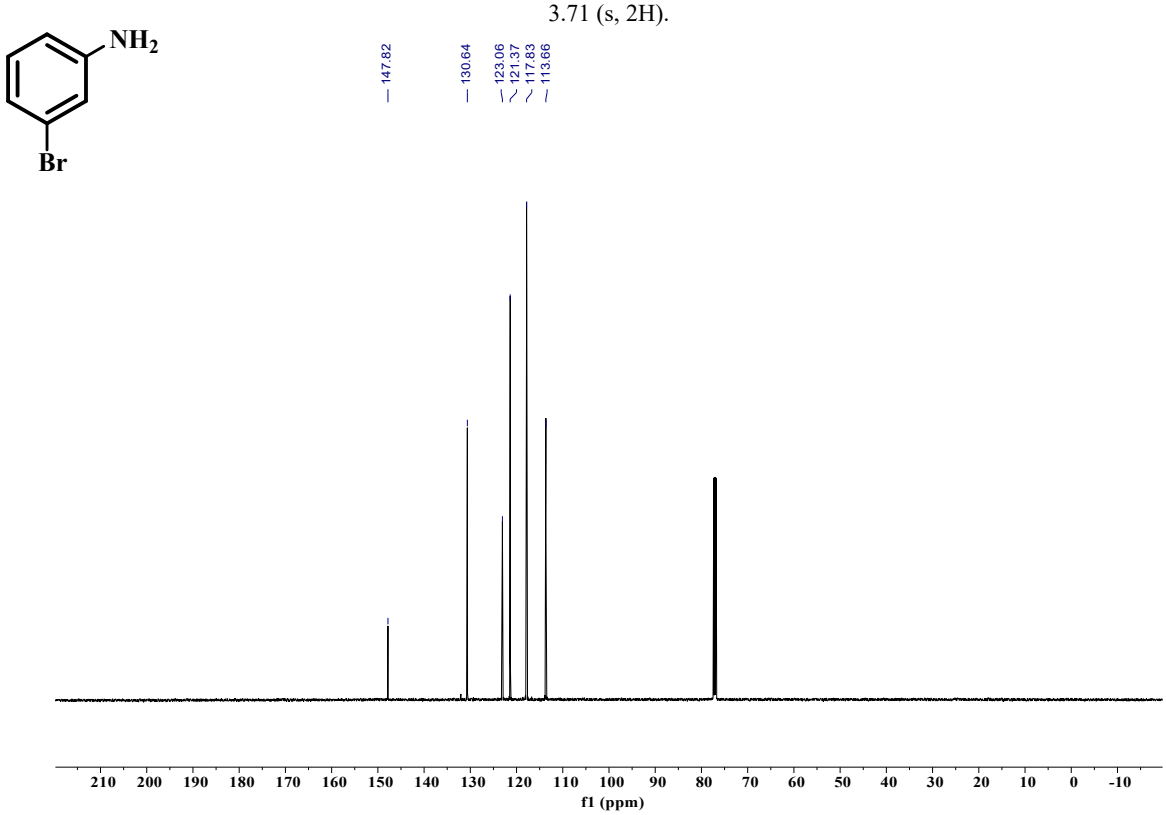

Figure. S30 ^{13}C NMR spectra of 2i (126 MHz, $CDCl_3$).
3–Bromoaniline (2k): ^{13}C NMR (126 MHz, Chloroform–d) δ 147.82(s), 130.64(s), 123.06(s), 121.37(s), 117.83(s), 113.66(s).

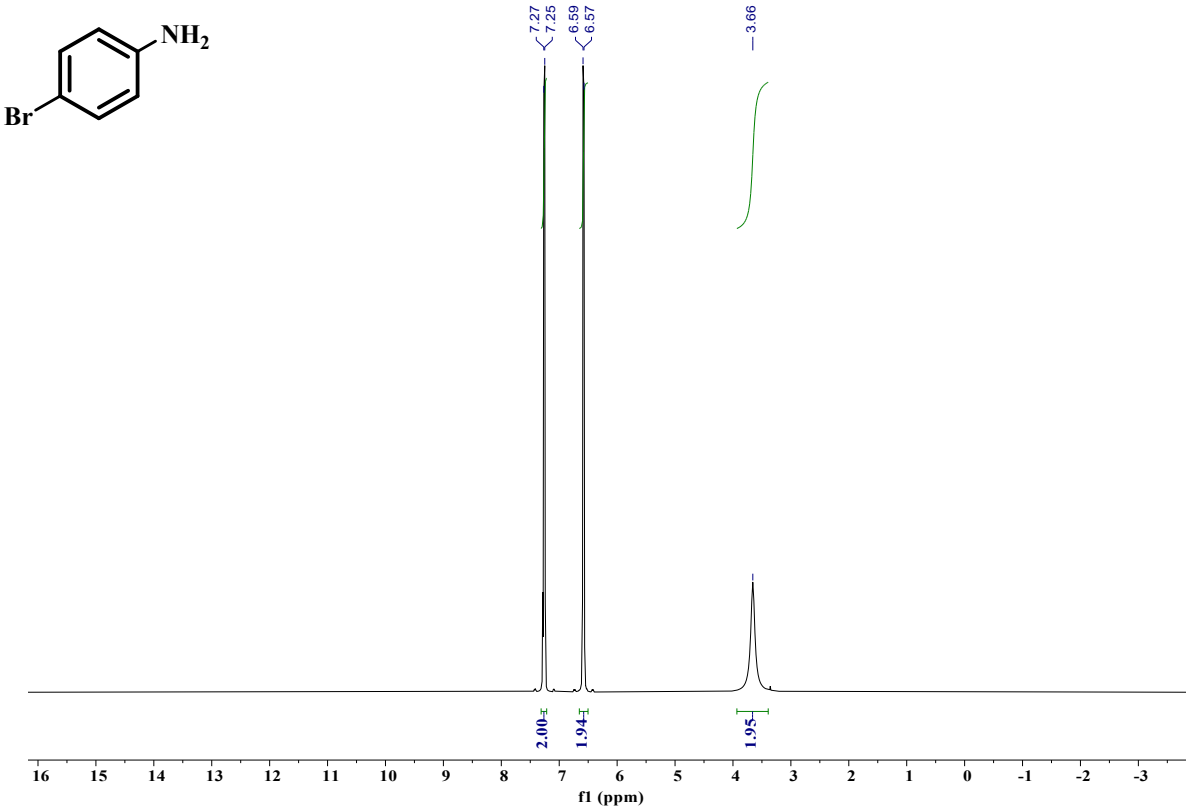

Figure. S31 ^{1}H NMR spectra of 2k (500 MHz, $CDCl_3$).
4–Bromoaniline (2l): ^{1}H NMR (500 MHz, Chloroform–d) δ 7.26 (d, J = 8.3 Hz, 2H), 6.58 (d, J = 8.3 Hz, 2H), 3.66 (s, 2H).

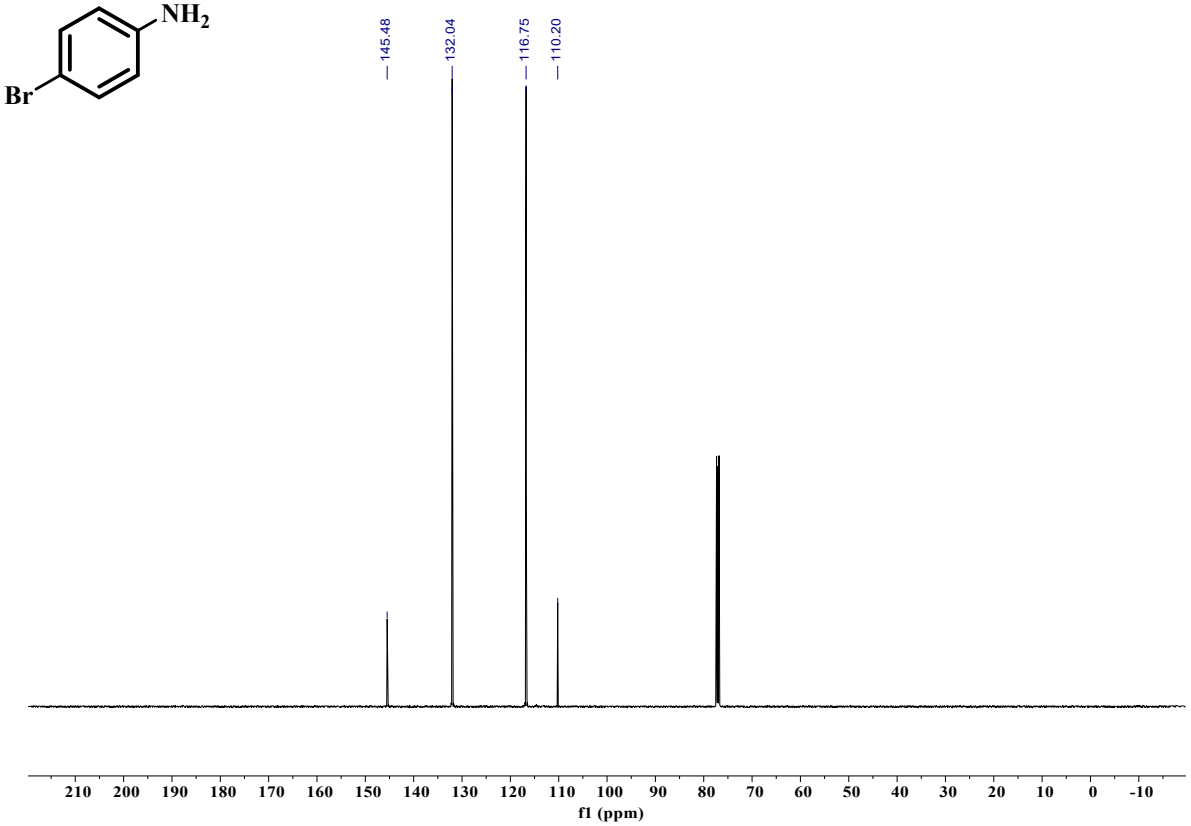

Figure. S32 ^{13}C NMR spectra of 2k (126 MHz, $CDCl_3$).
4–Bromoaniline (2l): ^{13}C NMR (126 MHz, Chloroform–d) δ 145.48(s), 132.04(s), 116.75(s), 110.20(s).

References

1 G. M. Sheldrick, *Acta Crystallogr. Sect. C Struct. Chem.*, 2015, **71**, 3–8.
2 O. Borbulevych, K. M. Merz Jr and L. M. Westerhoff, *Acta Crystallogr. A*, 2011, **67**, C593–C593.
3 Y. Sun, S. Zhang, M. Cai, P. Ma, J. Niu and J. Wang, *J. Mater. Chem. A*, 2024, **12**, 29580–29587.
4 W. Tang, Y. Liu, Y. Jin, Y. Wang, W. Shi, P. Ma, J. Niu and J. Wang, *Inorg. Chem.*, 2024, **63**, 6260–6267.
5 W. Chen, H. Li, Y. Jin, C. Wu, Z. Yuan, P. Ma, J. Wang and J. Niu, *Chem. Commun.*, 2022, **58**, 9902–9905.
6 J. Jiao, H. Sun, C. Si, J. Xu, T. Zhang and Q. Han, *ACS Appl. Mater. Interfaces*, 2022, **14**, 16386–16393.
7 S.-K. Shi, X. Li, H. Guo, Y. Fan, H. Li, D.-B. Dang and Y. Bai, *Inorg. Chem.*, 2020, **59**, 11213–11217.
8 H. Li, W. Chen, Z. Yuan, Y. Jin, Y. Zhao, P. Ma, J. Niu and J. Wang, *Inorg. Chem.*, 2022, **61**, 9935–9945.
9 C. Ren, Z. Lu, B. Luo, X. Yi, L. Lin and L. Xu, *Inorg. Chem. Front.*, 2021, **8**, 5178–5185.
10 Z. Tian, J. Han, F. Wu, X. Chen, D. Hu, F. Yu, K. Qi and W. Wang, *ChemistrySelect*, 2024, **9**, e202401545.
11 Y. Shi, H. Wang, Z. Wang, T. Wu, Y. Song, B. Guo and L. Wu, *J. Mater. Chem. A*, 2020, **8**, 18755–18766.
12 A. O. Moghanlou, M. H. Sadr, A. Bezaatpour, F. Salimi and M. Yosefi, *Mol. Catal.*, 2021, **516**, 111997.
13 Y. Xie, D. Liu, B. Wang, D. Li, Z. Yan, Y. Chen, J. Shen, Z. Zhang and X. Wang, *ACS Sustain. Chem. Eng.*, 2021, **9**, 2465–2474.